Biochemical characterization of two GH70 family 4,6-α-glucanotransferases with distinct product specificity from Lactobacillus aviarius subsp. aviarius DSM 20655

Meng, Xiangfeng; Gangoiti, Joana; de Kok, Niels; van Leeuwen, Sander S; Pijning, Tjaard; Dijkhuizen, Lubbert

Published in:
Food Chemistry

DOI:
10.1016/j.foodchem.2018.01.154

Publication date:
2018

Food Chemistry 253 (2018) 236–246

Contents lists available at ScienceDirect

Food Chemistry

journal homepage: www.elsevier.com/locate/foodchem

Biochemical characterization of two GH70 family 4,6-α-glucanotransferases with distinct product specificity from *Lactobacillus aviarius* subsp. *aviarius* DSM 20655

Xiangfeng Meng[a,b], Joana Gangoiti[b,1], Niels de Kok[b], Sander S. van Leeuwen[b], Tjaard Pijning[c], Lubbert Dijkhuizen[b,*]

[a] State Key Laboratory of Microbial Technology, School of Life Science, Shandong University, Shanda Nan Road 27#, 250100 Jinan, China
[b] Microbial Physiology,Groningen Biomolecular Sciences and Biotechnology Institute (GBB),University of Groningen,Nijenborgh 7,9747 AG Groningen,The Netherlands
[c] Biophysical Chemistry,Groningen Biomolecular Sciences and Biotechnology Institute (GBB),University of Groningen,Nijenborgh 7,9747 AG Groningen,The Netherlands

ARTICLE INFO

Keywords:
α-Glucan
4,6-α-Glucanotransferase
Family GH70
Lactic acid bacteria
Glucansucrase
Polysaccharides

ABSTRACT

Nine GtfB-like 4,6-α-glucanotransferases (4,6-α-GTs) (represented by GtfX of *L. aviarius* subsp. *aviarius* DSM 20655) were identified to show distinct characteristics in conserved motifs I-IV. In particular, the "fingerprint" Tyr in motif III of these nine GtfB-type 4,6-α-GTs was found to be replaced by a Trp. In *L. aviarius* subsp. *aviarius* DSM20655, a second GtfB-like protein (GtfY), containing the canonical GtfB Tyr residue in motif III, was located directly upstream of GtfX. Biochemical characterization revealed that both GtfX and GtfY showed GtfB-like 4,6-α-GT activity, cleaving (α1→4) linkages and catalyzing the synthesis of (α1→6) linkages. Nonetheless, they differ in product specificity; GtfY only synthesizes consecutive (α1→6) linkages, yielding linear α-glucan products, but GtfX catalyzes the synthesis of (α1→6) linkages predominantly at branch points (22%) rather than in linear segments (10%). The highly branched α-glucan produced by GtfX from amylose V is resistant to digestion by α-amylase, offering great potential as dietary fibers.

1. Introduction

Lactic acid bacteria are known to produce large amounts of exopolysaccharides (EPS), which are widely explored in the food industries as texturizer, viscosifier and emulsifier for the development of functional food (Badel, Bernardi, & Michaud, 2011; Ryan, Ross, Fitzgerald, Caplice, & Stanton, 2015; Zannini, Waters, Coffey, & Arendt, 2015). α-Glucan with various linkage composition [(α1→3), (α1→4) and (α1→6) linkages], degree of branching and size are synthesized from sucrose by GH70 glucansucrase enzymes with the successive transfer of glucosyl units to growing glucan chains in a linear or branching mode (Leemhuis, Pijning et al., 2013; Leemhuis, Pijning, Dobruchowska, Dijkstra, & Dijkhuizen, 2012; Monsan et al., 2001; Naessens, Cerdobbel, Soetaert, & Vandamme, 2005). Additionally, highly branched α-glucans can be synthesized by branching sucrases (i.e. DsrE-CD2 of *Leuconostoc mesenteroides* NRRL B-1299) (Brison et al., 2012; Vuillemin et al., 2016), a special subfamily of GH70 glucansucrase enzymes, which, in addition to the donor substrate sucrose, require a dextran acceptor substrate to which single glucosyl units are transferred via either (α1→2) or (α1→3) linkages (Brison, et al., 2012; Vuillemin, et al., 2016).

For a long time, glucansucrase enzymes constituted the single activity in the GH70 family. However, upstream of the glucansucrase GtfA [synthesizing α-glucans with (α1→4) linkages and (α1→6) linkages from sucrose] encoding gene in the *L. reuteri* 121 genome, a second glucansucrase-like enzyme (GtfB) is encoded (with 46% identity to GtfA) (Fig. S1) (Kralj et al., 2011). GtfB was found to be inactive on sucrose but rather uses malto-oligosaccharides (MOS) as substrate (Kralj et al., 2011). It predominantly cleaves (α1→4) linked glucosyl units in MOS substrates and transfer these to the non-reducing end of acceptor MOS with the formation of (α1→6) linkages in linear mode (Dobruchowska et al., 2012). Two more such enzymes from *Lactobacillus* strains, GtfW and GtfML4 were characterized later on (Leemhuis, Dijkman et al., 2013). GtfB type enzymes were therefore designated as 4,6-α-glucanotransferases (4,6-α-GTs), constituting a second subfamily within GH70 (Kralj et al., 2011; Leemhuis, Dijkman et al., 2013). GtfB was further shown to convert amylose and high-amylose starch into isomalto-/malto-polysaccharides (IMMP) with high (up to 91%) percentages of (α1→6) linkages (Leemhuis et al., 2014). Structural analysis

* Corresponding author at: CarbExplore Research BV, Zernikepark 12, 9747 AN Groningen, The Netherlands.
E-mail addresses: x.meng@sdu.edu.cn (X. Meng), j.gangoiti.munecas@rug.nl (J. Gangoiti), n.a.w.de.kok@rug.nl (N. de Kok), s.s.van.leeuwen@rug.nl (S.S. van Leeuwen), t.pijning@rug.nl (T. Pijning), l.dijkhuizen@rug.nl (L. Dijkhuizen).
[1] Current address: CarbExplore Research BV, Zernikepark 12, 9747 AN Groningen, The Netherlands.

https://doi.org/10.1016/j.foodchem.2018.01.154
Received 29 July 2017; Received in revised form 16 November 2017; Accepted 23 January 2018
Available online 31 January 2018

Bacterial strain	NCBI accesion numbers	Motif II		Motif III		Motif IV		Motif I	
A: Glucansucrases			3 4		5		6 7		1 2
Lactobacillus reuteri 180 (Gtf180)	AAU08001.1	1021	GIRVDAVDNVD	1058	HINILEDWGWD	1131	FVRAHDSNAQDQIRQ	1503	ADWVPDQ
Leuconostoc mesenteroides NRRL B-512F (DsrS)	AAD10952.1	547	GIRVDAVDNVD	584	HLSILEDWSHN	657	FVRAHDSEVQTVIAQ	1023	ADWVPDQ
Streptococcus oralis ATCC10557 (GtfR)	BAA95201.1	512	GVRVDAVDNVN	549	HLSILEAWSDN	622	FVRAHDSEVQTVIAD	1003	ADWVPDQ
Lactobacillus reuteri 121 (GtfA)	AAU08015.1	1020	SVRVDAPDNID	1056	HINILEDWNHA	1128	FVRAHDNNSQDQIQN	1508	ADWVPDQ
Lactobacillus reuteri ATCC 55730 (GtfO)	AAY86923.1	1020	SVRVDAPDNID	1056	HINILEDWNSS	1128	FIRAHDNNSQDQIQN	1508	ADWVPDQ
Streptococcus mutans SI (GtfC)	BAA26114.1	473	SIRVDAVDNVD	510	HLSILEAWSYN	582	FIRAHDSEVQDLIRD	954	ADWVPDQ
Leuconostoc citreum NRRL B-1355 (Asr)	CAB65910.2	631	GIRVDAVDNVD	668	HLSILEDWNGK	762	FVRAHDYDAQDPIRK	1168	ADWVPDQ
B: Branching Sucrases									
Leuconostoc citreum NRRL B-1299 (DsrE-CD2)	CAD22883.1	2206	SIRIDAVDFIH	2243	HISLVEAGLDA	2317	IIHAHDKGVQEKVGA	2688	ADVVDNQ
Leuconostoc citreum NRRL B-1299 (BRS-A)	CDX66896.1	668	SIRIDAVDFVS	705	HLSLVEAGLDA	779	IIHAHDKDIQDKVGA	1151	ADVVANQ
Lactobacillus kunkeei EFB6 (BRS-D)	WP_051592287.1	520	SIRIDAVDFIS	557	HISLVEGGVDA	638	IVHAHDKDVQEKVGQ	1010	ADVVYNQ
Leuconostoc citreum NRRL B-742 (BRS-B)	CDX65123.1	667	SMRIDAISFVD	704	HISIVEAPKGE	783	IVHAHDKDIQDTVIH	1182	ADFVANQ
Leuconostoc fallax KCTC 3537 (BRS-C)	WP_010006776.1	734	SIRIDAISFVD	771	HVSIVEASADQ	845	IVHAHDKDIQDAVSN	1232	ADYVANQ
C: Canonical GtfB-like proteins									
Lactobacillus reuteri 121 (GtfB)	AAU08014.2	1011	GFRVDAADNID	1048	HLSYNEGYHSG	1120	FVTNHDQR-KNLINR	1478	EDIVMNQ
Lactobacillus reuteri DSM 20016 (GtfW)	ABQ83597.1	748	GFRVDAADNID	785	HLVYNEGYHSG	858	FVTNHDQR-KNVINQ	1215	EDLVMNQ
Lactobacillus reuteri ML1 (GtfML4)	AAU08003.2	1012	GFRVDAADNID	1049	HLSYNEGYHSG	1121	FVTNHDQR-KNLINR	1479	EDIVMNQ
Pediococcus pentosaceus IE-3	CCG90643.1	380	GFRIDAADNID	417	HLSYNEGYHSG	489	FVTNHDQR-KNLINS	841	EDIVMNQ
Lactobacillus fermentum ATCC 14931	EEI21226.1	406	GFRIDAADNID	443	HLIYNEGYHSG	512	FVTNHDQR-KNLINQ	862	EDLVMNQ
Lactobacillus plantarum subsp. argentoratensis DSM 16365	KRL97280	265	GFRIDAADNID	302	HLSYNEGYHSG	374	FVTNHDQR-KNLINR	732	EDIVMNQ
Lactobacillus delbrueckii subsp. delbrueckii DSM 20074	WP_057717954.1	637	GFRVDAADNID	674	HLSYNEGYHSG	746	FVTNHDQR-KNLINR	1104	EDIVMNQ
Lactobacillus acidipiscis	KRN79505.1	402	GFRNDAADNID	439	HLVYNEGYHSG	508	FVTNHDQR-KNVINQ	867	VDMVMNQ
***Lactobacillus aviarius* subsp. aviarius DSM 20655 (GtfY)**	KRM39240.1	691	GFRVDAADNID	728	HLVYDESYHSN	801	FVNNHDQQ-KNIINQ	1153	VDLVMNQ
Lactobacillus fermentum NCC 2970	AQR73699.1	983	GFRIDAADDMD	1020	HLSYNEGYGPG	1092	YVTNHDIR-NNLING	1446	EDIVMNQ
D: GtfB-like proteins of interest									
***Lactobacillus aviarius* subsp. aviarius DSM 20655 (GtfX)**	KRM39239.1	701	GFRVDSASNMD	738	HLIYDEVWDPT	811	FVMNHDQR-ADIIKQ	1168	VDLVPNQ
Lactobacillus aviarius	WP_057827104	711	GFRVDSASNMD	748	HLIYDEVWDPT	821	FVMNHDQR-ADIIKQ	1178	VDLVPNQ
Lactobacillus aviarius	QAS74679.1	712	GFRVDSASNMD	749	HLIYDEVWDPN	822	FVMNHDQR-ADIIKQ	1179	VDLVPNQ
Lactobacillus aviarius	WP_064213164.1	702	GFRVDSASNMD	739	HLIYDEVWDPN	812	FVMNHDQR-ADIIKQ	1169	VDLVPNQ
Lactobacillus aviarius	WP_064208393.1	702	GFRVDSASNMD	739	HLIYDEVWDPN	812	FVMNHDQR-ADIIKQ	1169	VDLVPNQ
Lactobacillus aviarius	WP_064225342.1	712	GFRVDSASNMD	749	HLIYDEVWDPN	822	FVMNHDQR-ADIIKQ	1179	VDLVPNQ
Lactobacillus aviarius	WP_064214930.1	712	GFRVDSASNMD	749	HLIYDEVWDPN	822	FVMNHDQR-ADIIKQ	1179	VDLVPNQ
Lactobacillus aviarius	WP_064538564.1	702	GFRVDSASNMD	739	HLIYDEVWDPN	812	FVMNHDQR-ADIIKQ	1169	VDLVPNQ
Lactobacillus aviarius subsp. araffinosus DSM 20653	KRM53479.1	678	GLRVDAPDNID	715	HLVYTEAWDPT	794	FVMNHDQR-GDTIKQ	1149	VDFVPNQ
			-1 +1 +1		+1 +2		-1 +2 +2 -1		-1
			NU		A/B		TS		

Fig. 1. Amino acid sequence alignment of conserved motifs II, III, IV and I in the catalytic domain of GH70 glucansucrases (A), branching sucrases (B), GtfB-like proteins that contain a Trp at position 1065 (Gtf180 numbering) (C), and other GtfB-like proteins (D, E) that display variations in motif II, III, IV and I. The seven strictly conserved amino acid residues (indicated by the number 1–7) in GH70 family proteins are highlighted. The catalytic nucleophile (NU), general acid/base (A/B) and transition state stabilizing residues are highlighted in red. Residues forming the substrate binding sites −1, +1 and +2 are highlighted in color and indicated below. (For interpretation of the references to color in this figure legend, the reader is referred to the web version of this article.)

of the IMMP products showed that it constituted an entirely novel class of α-glucans, different from the known dextrans and isomalto-oligosaccharides. Notably, these IMMP are proven soluble dietary fibers since the segments rich in (α1→6) linkages are resistant to lytic α-amylases; therefore they largely pass the human small intestine and enter the large intestine (Leemhuis et al., 2014).

GtfB-like 4,6-α-GTs share high homology with glucansucrase enzymes and also contain their circularly permuted $(\beta/\alpha)_8$ barrel with the permuted order (II-III-IV-I) of conserved motifs compared to the closely related GH13 family enzymes (Kralj et al., 2011; Leemhuis, Dijkman et al., 2013; MacGregor, Jespersen, & Svensson, 1996). The seven highly conserved residues, including the catalytic residues (D1025, E1063 and D1136, Gtf180 numbering) of GH70 glucansucrases are also present in 4, 6-α-GTs (Fig. 1). On the other hand, some of the residues in GH70 homology motifs I-IV are not conserved in 4,6-α-GTs (Fig. 1); these regions are shown to be involved in donor/acceptor binding and hence in product specificity of glucansucrase enzymes (Leemhuis et al., 2012; Moulis et al., 2006). In particular, residue W1065 (Gtf180 numbering, motif III), which is highly conserved in GH70 GSs (except for branching sucrases), is replaced by a Tyr residue in GtfB-like 4,6-α-GTs (Meng et al., 2016). Considering the sequence similarity of GtfB-like 4,6-α-GTs with GH70 glucansucrases and their reaction similarity with GH13 family α-amylases, GtfB-like 4,6-α-GTs were proposed to represent a separate evolutionary intermediate subfamily of GH70 between GH13 family α-amylases and GH70 glucansucrases (Kralj et al., 2011; Meng et al., 2016); this was confirmed by structural and phylogenetic analyses and *in vivo* studies (Bai, Gangoiti, Dijkstra, Dijkhuizen, & Pijning, 2017).

Until recently, characterized GH70 GtfB-like proteins were only found to catalyze the synthesis of successive (α1→6) linkages using MOS and amylose as substrates, yielding linear IMMP or IMMO products (Kralj et al., 2011; Leemhuis, Dijkman et al., 2013; Leemhuis et al., 2014). In view of the diverse linkage specificity of GH70 glucansucrases, one may speculate that GH70 GtfB-like proteins also possess the ability to synthesize other linkage types besides the successive (α1→6) linkages, or even branched linkages. Indeed, a GtfB-like enzyme of *Lactobacillus fermentum* NCC2970, recently identified in the Nestlé Culture Collection (NCC), displayed a distinct linkage specificity by transferring glucosyl units via bridging and branching (α1→3) linkages; hence it was designated a 4,3-α-glucanotransferase (Gangoiti et al., 2017). In our present study, we report the identification of two adjacent gene products in *Lactobacillus aviarius* subsp. *aviarius* DSM 20655, both encoding GtfB-like 4,6-α-GT enzymes (GtfX and GtfY) with unique amino acid sequences in motifs I-IV. Biochemical characterization revealed that both GtfX and GtfY, similar to other GtfB-like enzymes, cleave (α1→4) linked glucosyl units of amylose. However, they differ in their product specificity; while GtfY mainly forms consecutive (α1→6) linkages at the non-reducing end, yielding linear IMMP or IMMO products in a similar fashion to other characterized GtfB-type enzymes, GtfX shows a novel specificity in the GtfB subfamily, mainly forming branching (α1→6) linkages onto (α1→4) glucan chains.

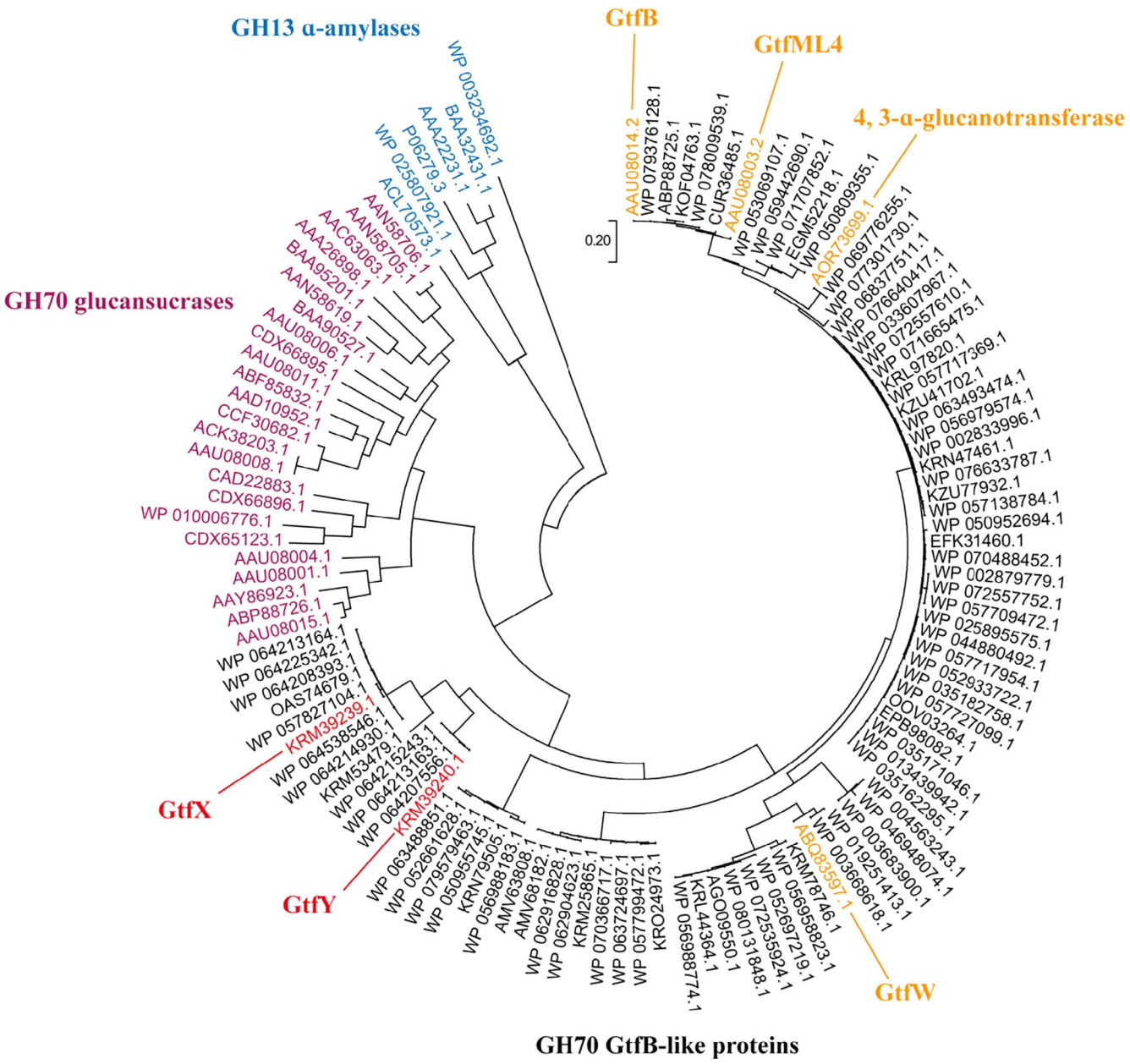

Fig. 2. Phylogenetic tree of 88 (putative) GtfB-like proteins (black) identified via Blastp searches using *L. reuteri* 121 GtfB as query sequence, 24 selected biochemically characterized glucansucrase enzymes (highlighted in magenta) and 6 selected characterized GH13 family α-amylases (highlighted in blue). Each sequence is labeled with its Genbank accession number. The bar corresponds to a genetic distance of 0.20 substitutions per position (20% amino acid sequence difference). The biochemically characterized GtfB-like proteins are highlighted in light brown. GtfX and GtfY characterized in the present study are highlighted in red. (For interpretation of the references to color in this figure legend, the reader is referred to the web version of this article.)

2. Materials and methods

2.1. Identification and sequence analysis of GtfB-like proteins

Eighty eight GtfB-like proteins in the non-redundant protein sequence database were identified by Blastp search as described in the Supplementary Material. A phylogenetic tree of these 88 (putative) GtfB-like proteins, 24 selected biochemically characterized glucansucrase enzymes and 6 selected GH13 α-amylases were constructed using the Maximum Likelihood method based on the JTT matrix model by MEGA version 7.0 (Kumar, Stecher, & Tamura, 2016). The positions containing alignment gaps and missing data were partially deleted. The statistical confidence of the inferred phylogenetic relationships was determined by conducting 1000 bootstrap replicates. The GenBank accession numbers of the sequences used in the phylogenetic analysis are visualized in Fig. 2.

Multiple amino acid sequence alignment of 88 (putative) GtfB-like proteins with selected biochemically characterized glucansucrase enzymes was performed using the MUSCLE web service with default parameters and visualized with Jalview (Waterhouse, Procter, Martin, Clamp, & Barton, 2009). Conserved motifs I, II, III and IV were identified according to the sequence alignments with biochemically characterized glucansucrases. The presence of a signal peptide and its cleavage site were predicted by Signal P4.1 web server (http://www.cbs.dtu.dk/services/SignalP/). The domain organization of candidate GtfB-like proteins were predicted by pairwise alignment with GtfB of *L. reuteri* 121, of which the three-dimensional structure is available (GtfB-ΔNΔV, Protein Data Bank code 5JBD) (Bai et al., 2017).

2.2. Cloning of the gtfX and gtfY genes of Lactobacillus aviarius subsp. aviarius DSM 20655

DNA fragments encoding domain IV, A, B and C of *gtfX* (GenBank accession number: KRM39239.1) and *gtf*Y (KRM39240.1) were amplified from *L. aviarius* subsp. *aviarius* DSM 20655 genomic DNA, resulting in the cloning of GtfX-ΔNΔC (amino acids 448–1304) and GtfY-ΔNΔC (amino acids 438–1290). Phusion DNA polymerase (Finnzyme, Helsinki, Finland) was used to facilitate high-fidelity DNA amplification. The resulting PCR products were cloned into a modified pET15b vector (pET15b-LIC) using a ligase independent cloning (LIC) technique as previously described (Gangoiti, et al., 2017). The primers for the cloning of *gtf*X-ΔNΔC were: Forward 5′-CAGGGACCCGGTGCCTTAGA AACTTATTCTGGGGATG-3′ and Reverse 5′-CGAGGAGAAGCCCGGTTA TGTGAATTGAGCCGGCAACG-3′; Primers for the cloning of *gtf*Y-ΔNΔC were: Forward 5′-CAGGGACCCGGTGCGCTTGAAATGTACCGTGGAA ATG-3′ and Reverse: 5′-CGAGGAGAAGCCCGGTTAGGTAAATTGGGTC GGAACAGTTG-3′.

2.3. Recombinant protein expression and purification

The 5 ml overnight cultures of *E. coli* BL21 (DE3) star strains containing appropriate plasmid constructs were inoculated in 500 ml Studier's auto-induction (AI) media (Studier, 2014) with 1.0% glycerol and 0.1% lactose (w/v) as carbon source and 100 μg/ml ampicillin. The culture was further incubated at 20 °C for 30 h. The cells were harvested by centrifugation at 9500 × *g* for 10 min at 4 °C and lysed using bacterial protein extraction reagent (B-PER) (Thermo Scientific, Pierce). Cell-free-extract (CFE) supernatants were obtained by centrifugation (27,000 × *g*) at 4 °C for 20 min. The recombinant GtfX-ΔNΔC and GtfY-ΔNΔC proteins were purified from CFE by Ni^{2+}-nitrilotriacetic acid (NTA) (Sigma-Aldrich) affinity chromatography. The purified proteins were desalted in 50 mM sodium acetate buffer 1 mM $CaCl_2$ pH 5.75 buffer using an ultrafiltration unit (Amicon, Beverly, MA) with a 50,000 molecular weight cut off. The purity and homogeneity of purified protein fraction were analyzed on SDS-PAGE and the concentration was determined using a Nanodrop 2000 spectrophotometer (Isogen Life Science, De Meern, The Netherlands) by measuring the absorbance at 280 nm.

2.4. Enzyme activity assays

The initial activities of GtfX and GtfY were determined using an amylose-iodine activity assay as described previously (Bai et al., 2015). Briefly, the reaction mixture contained 0.125% (w/v) amylose V (AVEBE, Foxhol, The Netherlands) as substrates. The decrease of the absorbance at 660 nm of the α-glucan-iodine complex was monitored with the progress of reaction time by adding iodine-staining solution. One unit of enzyme activity was defined as the converting 1 mg of substrate per min. The effects of pH on enzyme activity were performed at 30 °C using 5–20 μg/ml of purified enzyme in various buffers ranging from pH 2.5–7.0. All buffers had a concentration of 50 mM and were supplemented with 1 mM $CaCl_2$. The buffers used include glycine-HCl (pH 2.5–3.5), sodium acetate (pH 3.5–5.5) and MES (pH 5.5–7.0). The optimum temperature was determined in sodium acetate buffer with the optimum pH values previously determined (GtfX-ΔNΔC at pH 4.0 and GtfY-ΔNΔC at pH 5.0) at various temperatures ranging from 30 to 78 °C. All activity assays were performed in duplicate. To evaluate the thermostability of the enzyme, thermofluor assays were performed to determine the T_m of each enzyme as previously described (Bultema, Kuipers, & Dijkhuizen, 2014).

2.5. Substrate specificity analysis of GtfX-ΔNΔC and GtfY-ΔNΔC

The purified GtfX-ΔNΔC and GtfY-ΔNΔC enzymes (20 μg/ml) were separately incubated with amylose V (AVEBE), amylopectin (Sigma-Aldrich), potato starch (Sigma-Aldrich), dextran (10.6 KDa avg. MW, Sigma-Aldrich) and pullulan at a concentration of 0.6%. Oligosaccharides including MOS with different degree of polymerization (DP2 to 7) (Sigma-Aldrich), sucrose (Acros), nigerose (Sigma-Aldrich), panose (Sigma-Aldrich), isomaltose (i-G2, Sigma-Aldrich), isomaltotriose (i-G3, Sigma-Aldrich) and α-cyclodextrin (Fluka) were used as substrates at a concentration of 25 mM. All reactions were performed in 50 mM sodium acetate buffer 1 mM $CaCl_2$ with the optimum pH value for the respective enzyme (GtfX-ΔNΔC at pH 4.0 and GtfY-ΔNΔC at pH 5.0). The reaction mixtures were incubated at 37 °C for 48 h for the amylose V, starch, dextran and pullulan substrates and for 24 h for the other substrates. This was followed by inactivation of the enzymes by heating samples at 95 °C for 10 min. The reaction mixture products were analyzed using thin-layer chromatography (TLC) as previously described (Meng, Pijning, Dobruchowska, Gerwig, & Dijkhuizen, 2015).

2.6. High-performance anion-exchange chromatography (HPAEC-PAD)

Product mixtures were analyzed by HPAEC on an ICS-3000 workstation (Dionex, Amsterdam, The Netherlands), equipped with an ICS-3000 ED pulsed amperometric detection (PAD) system. Samples of reaction products were diluted 1:100 in MilliQ water and separated on a CarboPac PA-1 column (Dionex, 250 × 4 mm) using a linear gradient of 10–240 mM sodium acetate in 100 mM NaOH over 57 min at a flow rate of 0.25 ml/min. The injection volume for each sample was 5 μl. The identity of some peaks was assigned using standard oligosaccharides.

2.7. Incubation of GtfX-ΔNΔC and GtfY-ΔNΔC with maltoheptaose and amylose V as substrates

Purified GtfX-ΔNΔC and GtfY-ΔNΔC enzymes (20 μg/ml) were incubated with 25 mM maltoheptaose and 0.6% amylose V at 37 °C in 50 mM sodium acetate buffer with respective optimum pH values. Reactions were followed in time by taking samples at 0, 10 min, 2 h and 8 h for maltoheptaose and at 0, 5 min, 1 h and 8 h for amylose V. The aliquot samples were immediately inactivated by heating at 95 °C for 10 min. The oligosaccharide products were analyzed by HPAEC-PAD.

Large scale incubations (50 ml) of GtfX-ΔNΔC and GtfY-ΔNΔC (20 μg/ml) with 0.6% amylose V were lyophilized and the polysaccharide fraction of product mixtures was isolated using a Bio-Gel P2 column (50 × 2.5 cm; Bio-Rad, Veenendaal, The Netherlands) by collecting the void volume fractions. The eluent used was 10 mM NH_4HCO_3 at a flow rate of 48 ml/h. The polysaccharide fractions were lyophilized and used for further structural analysis.

2.8. Structural analysis of products formed by GtfX-ΔNΔC and GtfY-ΔNΔC

Reaction product mixtures were exchanged twice in D_2O (99.9% atom; Cambridge Isotope Laboratories, Inc., Andover, MA) with intermediate lyophilization and re-dissolved in 600 μl D_2O. One-dimensional ^1H NMR spectra of the reaction products and isolated polysaccharide fractions were recorded in D_2O on a Varian Inova 500 spectrometer (NMR center, University of Groningen) at a probe temperature of 298 K. The ratio of different glycosidic linkage was determined by integration the surface area of respective signal peaks in the ^1H NMR spectra. 2D ^1H–^1H COSY, 2D ^1H–^1H TCOSY, 2D ^1H–^1H ROESY, 2D ^1C–^1H HSQC spectra were recorded and processed as previously described (Meng et al., 2017). The substitution pattern of polysaccharides was determined by methylation analysis as previously described (Ciucanu & Kerek, 1984).

2.9. Enzymatic digestion of polysaccharides produced by GtfX-ΔNΔC and GtfY-ΔNΔC from amylose V

Samples of isolated polysaccharides (5 mg/ml) were digested by

incubation with an excess amount of α-amylase of *Aspergillus oryzae* (Megazyme, Bray, Ireland), dextranase of *Chaetomium erraticum* (Sigma-Aldrich) or pullulanase M1 of *Klebsiella planticola* (Megazyme). Amylose V, dextran and pullulan were used as positive controls for α-amylase, dextranase and pullulanase M1 digestion, respectively. The enzymatic hydrolysis was performed in 50 mM sodium acetate buffer, pH 5.0 for 72 h. The generated digestion mixtures were analyzed by TLC and/or HPAEC.

2.10. Homology modeling

Homology models of the GtfX and GtfY protein structures were obtained with the Phyre server (Kelley, Mezulis, Yates, Wass, & Sternberg, 2015) with a multi-template/*ab initio* intensive protocol.

3. Results and discussion

3.1. Identification of two putative GtfB-like 4,6-α-GTs encoded by *Lactobacillus aviarius subsp. aviarius DSM 20655*

A Blastp search using the GtfB of *L. reuteri* 121 as query sequence resulted in the identification of 88 (putative) GtfB-like proteins from the NCBI non-redundant protein sequence database. Of these, 76 are encoded in *Lactobacillus* genomes and 10 in *Pediococcus* strains; one GtfB-like protein was found in *Leuconostoc mesenteroides* (GenBank accession number WP_059442690.1) and one in *Weissella confusa* (WP_071707852.1). GtfB-like proteins thus are not only found in *Lactobacillus* strains but also in other lactic acid bacteria. Whereas most GtfB-like proteins were found in *Lactobacillus* strains, glucansucrases are widespread in lactic acid bacteria, including *Leuconostoc*, *Lactobacillus*, *Streptococcus*, *Weissella* and *Oenococcus* (Meng et al., 2016). The reason for the more specific distribution of GtfB-like enzymes in *Lactobacillus* strains remains unknown. Phylogenetic analysis of the 88 (putative) GtfB-like enzymes, selected GH70 glucansucrases and GH13 α-amylases revealed that the putative GtfB-like enzymes form a separate cluster (Fig. 2), being defined as a separate GH70 subfamily previously (Kralj et al., 2011). Similar to the situation in the closely related glucansucrases, the different product linkage specificities of GtfB-type enzymes are likely the result of amino acid differences in acceptor binding regions (Leemhuis et al., 2012), which are mainly located in motifs I-IV (Fig. 1). We therefore aimed at finding GtfB-type enzymes with variations in these motifs; such enzymes may synthesize α-glucans from starch with different (desired) physicochemical properties.

Within the set of 88 putative GtfB-like proteins, nine putative GtfB-like proteins (all from *L. aviarius*) with variations at certain positions in motifs I-IV drew our attentions. First of all, these nine putative GtfB-like proteins (all from *L. aviarius*) contain a Trp residue in motif III, similar to glucansucrase enzymes (W1065, Gtf180 numbering). However, in previously identified GtfB-like proteins, it is replaced by a Tyr (Meng et al., 2016), as it is in 79 of the 88 proteins in the current study (including the 4,3-α-gluanotransferase of *L. fermentum* NCC2970). The conserved Trp residue in GH70 glucansucrase was shown to be critical for their polysaccharide synthesizing ability by providing stacking interactions with an acceptor substrate (Meng et al., 2017). In branching sucrases, this Trp residue is replaced by Gly, Pro or Ser (Brison et al., 2012; Vuillemin et al., 2016). Secondly, residues in motif IV following the transition state stabilizing residue (D1135, Gtf180 numbering) are involved in the formation of subsite +2 in glucansucrase enzymes and have been shown to contribute to product linkage specificity (Côté & Skory, 2014; Hellmuth2008; Leemhuis et al., 2012; Moulis, et al., 2006; Vujičić-Žagar et al., 2010). GtfB-like proteins differ from glucansucrases in this motif, and have a gap at position 1139 (Gtf180 numbering). Most GtfB-like proteins, including those forming successive (α1→6) linkages (GtfB, GtfW and GtfML4), contain QR-KN at position 1136, 1137, 1138 and 1140 (Gtf180 numbering), respectively (Fig. 1). The 4,3-α-glucanotransferase of *L. fermentum* NCC 2970 has IR-NN (Fig. 1), suggesting that also in the GtfB subfamily differences in motif IV may affect product linkage specificity. Interestingly, the nine putative GtfB-like proteins containing a Trp in motif III (Group D in Fig. 1) also show distinct amino acid sequences in motif IV. Eight out of nine have QR-AD while one (KRM53479.1 of *L. aviarius* subsp. *araffinosus* DSM 20653) has QR-GD. Finally, the third variation within GtfB-like enzymes is in motif II, at the positions corresponding to residues D1028 and N1029 (Gtf180 numbering). In Gtf180 of *L. reuteri* 180, this Asp/Asn pair provides direct and/or water-mediated hydrogen bonds to the C4 and C3 hydroxyl groups of the glucosyl moiety of the acceptor maltose at subsite +1 (Meng et al., 2015; Vujičić-Žagar et al., 2010). In most of the GtfB-like proteins, the Asp/Asn pair was found to be conserved; however, in GtfB-like proteins containing a Trp in motif III (except for KRM53479.1 of *L. aviarius* subsp. *araffinosus* DSM 20653), the Asp residue is replaced by a Ser residue.

Taken together, the nine putative GtfB-like proteins represented by KRM39239.1 show notable variations in motifs II-IV with respect to characterized GtfB-like enzymes with 4,6-α-GT specificity. Specifically, motifs II-IV of these putative GtfB-like proteins from *L. aviarius* either resemble the glucansucrases (motif III), show conservation with canonical GtfB-type 4,6-α-GTs (motif IV), or have a unique mutation (motif II). Given the importance of these regions for acceptor binding specificity in other GH70 enzymes, these enzymes may display novel reaction and product specificities. The nine proteins (group D in Fig. 1) show high sequence identity to each other [> 97% sequence identity except for KRM53479.1 (71% identity)]; we therefore chose KRM39239.1 (designated GtfX) from *L. aviarius* subsp. *aviarius* DSM 20655 as a representative of this group and performed further sequence and biochemical analysis. Interestingly, immediately upstream of KRM39239.1, another GtfB-like protein is present (KRM39240.1, designated GtfY) (Fig. S1). GtfY has a conserved Asp/Asn pair in motif II, and a Tyr residue in motif III, similar to GtfB-like 4,6-α-GT enzymes; in motif IV; the Arg at position 1138 is replaced by Gln. The adjacent location of GtfX and GtfY is reminiscent of the situation in *L. reuteri* 121, in which a tandem GtfA and GtfB with different reaction specificities (glucansucrase and 4,6-α-GT, respectively) are encoded (Kralj et al., 2004; Kralj et al., 2011); this further raised our interest to clone, express and biochemically characterize both GtfX and GtfY, providing new insights in the structure-function relationships of GH70 enzymes.

3.2. Analysis of the GtfX and GtfY protein sequence

The full sequences of GftX and GtfY comprise 1691 and 1567 amino acids, and share 68% identity, and 52% and 59% identity with GtfB of *L. reuteri* 121, respectively. Both enzymes encode a conserved Gram-positive signal peptide of 26 and 36 amino acids, indicating their extracellular location. Conserved domain analysis revealed that both GtfX and GtfY contain the catalytic core of the GH70 family. Recently, the first crystal structure of a 4,6-α-GT enzyme (GtfB-ΔNΔV of *L. reuteri* 121) has been reported (Bai et al., 2017). Like in glucansucrase enzymes, the polypeptide chain of GtfB-ΔNΔV takes a “U” course to form domains IV, B, A and C (IVn-Bn-An-C-Ac-Bc-IVc). Pairwise alignment of GtfX and GtfY with GtfB of *L. reuteri* 121 revealed the same domain organization and allowed the identification of domains IV, B, A and C (Fig. S2). The putative catalytic residues of GtfX and GtfY in motifs II, III and IV are Asp705/Glu743/Asp816 and Asp695/Glu733/Asp806, respectively. The N-terminal regions of GtfX and GtfY are shorter than in GtfB (about 420–430 instead of about 760 amino acids); however, GtfX and GtfY possess an extra region C-terminal of IVc (390 and 280 amino acids, respectively) which is absent in GtfB. Similar to other GH70 glucansucrase and 4,6-α-GT enzymes, the N- and C-terminal regions of GtfX and GtfY contain mainly amino acid repeats that are rich in YG repeats and are probably involved in glucan binding (Giffard & Jacques, 1994; Kralj, van Geel-Schutten, Dondorff et al., 2004; Kralj, van Geel-Schutten, van der Maarel et al., 2004; Monchois, Willemot, &

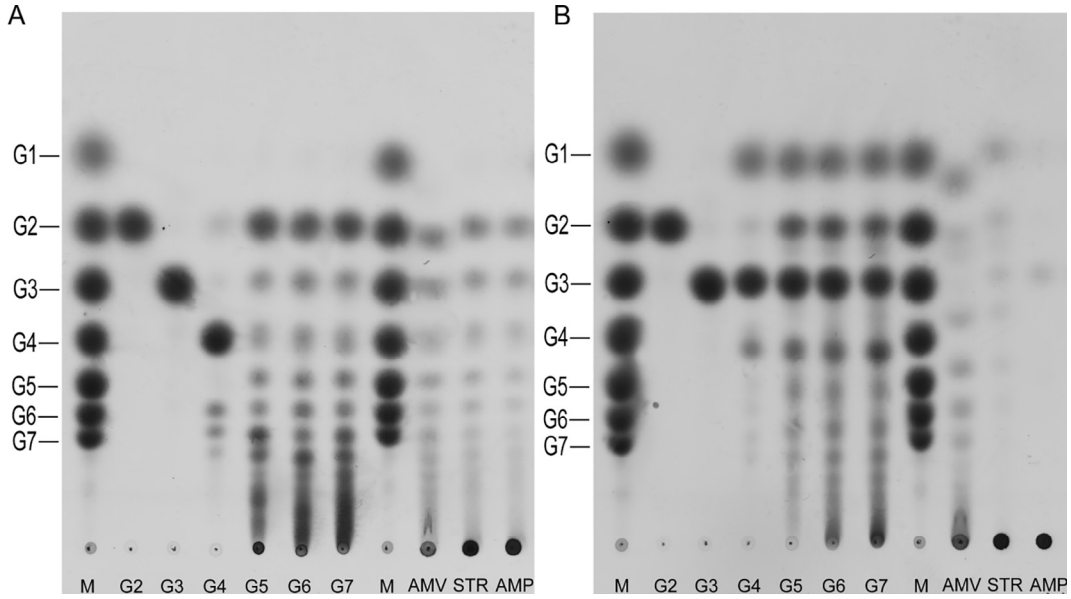

Fig. 3. TLC analysis of the products formed by incubation of 20 μg/ml GtfX-ΔNΔC (A) and GtfY-ΔNΔC (B) with MOS (DP2 to DP7), amylose V, potato starch and amylopectin. The reactions were performed at 37 °C in 50 mM sodium acetate buffer pH 4.0 (GtfX-ΔNΔC) and pH 5.0 (GtfY-ΔNΔC) for 24 h. M, standards; G1, glucose; G2, maltose; G3, maltotriose; G4, maltotetraose; G5, maltopentaose; G6, maltohexaose; G7, maltoheptaose; AMV, amylose V; STR, potato starch; AMP, amylopectin.

Monsan, 1999).

3.3. Cloning, purification, substrate specificity and biochemical properties of GtfX and GtfY enzyme

Previously, truncation of the N-terminal variable domain of *L. reuteri* 121 GtfB did not significantly affect its reaction and product specificity (Bai et al., 2017). To facilitate their expression, truncated constructs of GtfX and GtfY, GtfX-ΔNΔC (encoding residues 448–1304) and GtfY-ΔNΔC (encoding residues 438–1290), were cloned and expressed in *E. coli* BL21 (DE3) star. Recombinant GtfX-ΔNΔC and GtfY-ΔNΔC were purified from the soluble fraction of cell extracts by Ni^{2+}-NTA affinity chromatography. SDS-PAGE analysis showed that the molecular mass of both GtfX-ΔNΔC and GtfY-ΔNΔC is about 100 kDa (Fig. S3), in agreement with the predicted molecular mass (98 kDa).

The purified GtfX-ΔNΔC and GtfY-ΔNΔC proteins were incubated with different oligosaccharides and polysaccharides to explore their substrate specificity. Both GtfX-ΔNΔC and GtfY-ΔNΔC were inactive on sucrose, panose, nigerose, isomaltose, isomaltotriose, maltose, maltotriose, α-cyclodextrin, pullulan and dextran (Figs. 3 and S4) but showed clear hydrolase/transglycosylase activity on MOS of DP4-7, amylose V, starch and amylopectin (Fig. 3). Using amylose V as substrate, the pH and temperature profiles of GtfX-ΔNΔC and GtfY-ΔNΔC were determined (Fig. S5). GtfX-ΔNΔC retained more than 60% of its activity over a pH range from 3.0 to 7.0 and showed maximum activity at pH 4.0 (Fig. S5), similar to the biochemically characterized GtfB-like 4,6-α-GTs and 4,3-α-GT (Bai et al., 2015; Gangoiti et al., 2017). GtfX-ΔNΔC also retained more than 60% of its activity over a temperature range from 30 to 55 °C, showing maximum activity at 53 °C. Similarly, GtfY-ΔNΔC also showed broad pH tolerance, retaining more than 60% of activity from pH 2.5 to 5.5 and showing maximum activity at pH 5.0. GtfY-ΔNΔC retained more than 90% of its activity over a range of temperatures from 58 to 73 °C with an optimum temperature at 62 °C, which may suggest a higher thermostability compared to GtfX-ΔNΔC and other biochemically characterized GtfB-like proteins (Bai et al., 2015; Gangoiti et al., 2017; Leemhuis, Dijkman et al., 2013). This was confirmed by a thermofluor assay, revealing T_m values of 60 °C for GtfX-ΔNΔC and 71 °C for GtfY-ΔNΔC. The specific activities of GtfX-ΔNΔC and GtfY-ΔNΔC at optimum pH and temperature on 0.125% (w/v) amylose V were 17.9 U/mg and 19.6 U/mg, respectively. These values are similar to that of 4,3-α-GT of *L. fermentum* NCC 2970 (22.0 U/mg) (Gangoiti et al., 2017), but significantly higher than that of *L. reuteri* 121 GtfB (2.8 U/mg) (Bai et al., 2015).

TLC analysis showed that both GtfX-ΔNΔC and GtfY-ΔNΔC are inactive on maltose and maltotriose, but formed shorter as well as longer products from MOS of DP4-7 (Fig. 3), although the activity on maltotetraose (DP4) was minor. The observation that GtfX-ΔNΔC and GtfY-ΔNΔC require at least maltotetraose (DP4) as glucose donor substrate suggests that their donor substrate binding sites are different from other characterized 4,6-α-GTs that are active on MOS starting from DP3 (GtfB) (Dobruchowska et al., 2012) or DP2 (GtfW, GtfML4) (Leemhuis, Dijkman et al., 2013). GtfX-ΔNΔC and GtfY-ΔNΔC synthesized polymers when the enzymes were incubated with MOS above DP5 (Fig. 3). With amylose V, starch and amylopectin as substrates, they also produced oligosaccharides and polysaccharides (Fig. 3). Compared to GtfX-ΔNΔC, GtfY-ΔNΔC was less hydrolytically active on amylopectin in view of the small amount of oligosaccharides being formed. Similar to GtfB of *L. reuteri* 121, incubations of GtfY-ΔNΔC with MOS DP4-7, amylose V, starch or amylopectin produced glucose as hydrolysis product (Kralj et al., 2011); in contrast, incubation of GtfX-ΔNΔC with these substrates yielded maltose, suggesting that the latter enzyme employs a different mode of action.

3.4. ^{1}H NMR analysis of products formed by GtfX-ΔNΔC and GtfY-ΔNΔC

To explore the product specificity of GtfX-ΔNΔC and GtfY-ΔNΔC, ^{1}H NMR analysis was performed with the product mixtures obtained from MOS DP3-7, amylose V, starch and amylopectin. As an example, the ^{1}H NMR spectra of the product mixtures from amylose V are depicted in Fig. 4. In case of GtfX-ΔNΔC, the spectrum shows two broad anomeric signals at δ ~ 5.40–5.36 and δ ~ 4.97, suggesting the presence of (α1→4) and (α1→6) linkages, respectively (van Leeuwen, Leeflang et al., 2008). The anomeric signal at δ ~ 5.36 suggests the presence of -(1→4,6)-α-D-Glc*p*- branch points in the synthesized products (van Leeuwen et al., 2008), which is further supported by the relative high intensity of the H-4 signal (t4 between ~3.40–3.45) stemming from the terminal residues (Fig. 4) (van Leeuwen, Leeflang et al., 2008). The anomeric signals of Rα at δ 5.229 and Rβ at 4.658 demonstrate the presence of 4-substituted reducing-end glucose residues (van Leeuwen, Leeflang et al., 2008). The anomeric signals of free glucose (Gα at δ

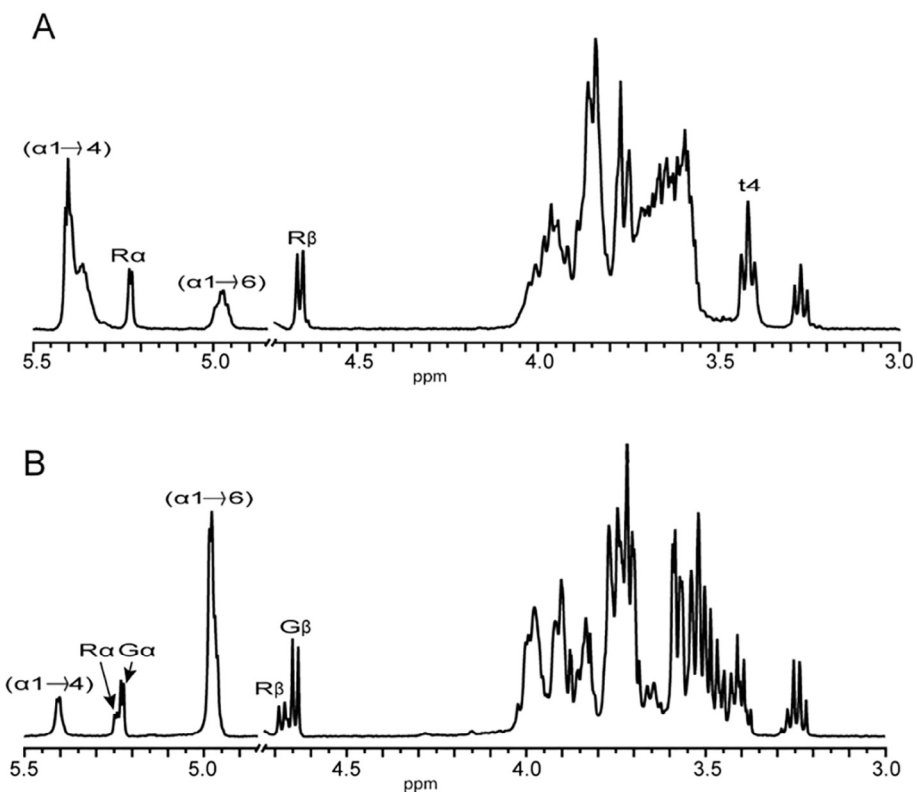

Fig. 4. ^{1}H NMR spectra of product mixtures obtained from amylose V incubations with GtfX-ΔNΔC (A) and GtfY-ΔNΔC (B) recorded in D_2O at 298 k. The signals corresponding to (α1→4) and (α1→6) linkages at δ ~ 5.40 and δ ~ 4.97, respectively, are indicated. Rα at δ 5.246 and Rβ at δ 4.679 correspond to the anomeric signal of reducing end glucose unit. Gα at δ 5.227 and Gβ at δ 4.642 originate from the anomeric proton of free glucose. The signal between δ ~ 3.40 and 3.45 (t4) is indicative of branched residues.

5.227, Gβ at δ 4.642) were not observed in the product mixture from incubating GtfX-ΔNΔC with amylose V, in agreement with our TLC analysis. Integration of the respective (α1→4) and (α1→6) anomeric signals showed that newly synthesized (α1→6) linked glucosyl units constitute about 18% of the product mixture. For GtfY-ΔNΔC, incubation with amylose V also resulted in anomeric signals at δ ~5.40 and δ ~4.97, suggesting the presence of (α1→4) and (α1→6) linkages, respectively. However, in contrast to GtfX-ΔNΔC, an anomeric signal at δ ~5.36 is absent, indicating that there are no detectable levels of -(1→4,6)-α-d-Glc*p*-(1→4)- branch points in synthesized products. Integration of the anomeric signals at δ ~5.40 and δ ~4.97 revealed that the product mixture contains 15% (α1→4) linked and 85% (α1→6) linked glucosyl units. Thus, the product profile of GtfY-ΔNΔC upon incubation with amylose V is similar to that of *L. reuteri* 121 GtfB, which comprises mainly consecutive (α1→6) linkages attached to the non-reducing end of malto-oligosaccharide units (IMMO or IMMP) (Dobruchowska et al., 2012; Leemhuis et al., 2014). The presence of anomeric signals of free glucose units (Gα at δ 5.227; Gβ at δ 4.642) is in accordance with our TLC analysis. Finally, the presence of anomeric signals corresponding to 6-substitued (Rα at δ 5.246, Rβ at δ 4.679) reducing-end glucose units suggests that the generated glucose units are also used as acceptor substrates and elongated with (α1→6)-linked glucosyl units.

The ratio of (α1→6) and (α1→4) linkages in the product mixtures from different substrates were obtained by the integration of the surface area of respective signal peaks in the ^{1}H NMR spectra (Fig. S6). When only linear (α1→4)-linked substrates (MOS DP4-7 and amylose V) are considered, the percentage of (α1→6) linkage in the product mixture of GtfY-ΔNΔC incubations increased with the size of the substrates, up to 85% with amylose V as substrate. In contrast, for GtfX-ΔNΔC no such trend was observed; all tested MOS substrates (DP5-7 and amylose V) yielded 16–18% (α1→6) linkages in the products, except with maltotetraose (DP4) for which the relative amount of (α1→6) linkages is only 3%, likely due to the minor activity on this substrate. GtfX-ΔNΔC also introduced a relatively high percentage of (α1→6) linkages in the product mixture with potato starch (13%) and amylopectin (12%). With GtfY-ΔNΔC, about the same relative amount (14%) was observed when incubated with potato starch; however, with amylopectin, the relative amount of (α1→6) linkages is considerably lower (3%), in agreement with its minor activity on this substrate as shown by TLC analysis. These results indicate that GtfY-ΔNΔC prefers linear (α1→4) linked glucans (MOS or amylose V) as substrates, similar to GtfB of *L. reuteri* 121 (Leemhuis et al., 2014); thus these two enzymes may employ a similar mode of action on these substrates.

3.5. Structural analysis of polysaccharides generated by GtfX-ΔNΔC and GtfY-ΔNΔC from amylose V

NMR analysis showed that the polysaccharide synthesized by GtfY-ΔNΔC has typical signals of successive (α1→6) linkages (δ 4.981) with (α1→4) linked MOS moieties present at the reducing end (Fig. S7); the percentages of (α1→6) linkages and (α1→4) linkages are 85% and 15%, respectively. Thus, GtfY-ΔNΔC catalyzes the synthesis of IMMP products, similar to those produced by GtfB of *L. reuteri* 121 (Dobruchowska et al., 2012). For the polysaccharides synthesized by GtfX-ΔNΔC, broad signals are present at δ ~ 5.40–5.36 [(α1→4) linkage] and δ ~ 4.97 [(α1→6) linkage] (Fig. S8), the percentages of which are 71% and 29%, respectively. The high intensity of the H-4 signal (t4 between δ ~ 3.40–3.45) stemming from the terminal residues suggests the presence of a high amount of branch points [-(1 → 4,6)-α-D-Glc*p*-], in agreement with our NMR analysis of the product mixtures. The structure of the polysaccharides produced by GtfX-ΔNΔC was further analyzed in detail by methylation analysis and 2D NMR analysis (Fig. S8). Methylation analysis revealed the presence of terminal [Glc*p*(1→], 4-substituted [→4)Glc*p*(1→], 6-substituted [→6)Glc*p*(1→] and 4,6-substituted [→4,6)Glc*p*(1→] glucosyl units in a molar ratio of 19%, 49%, 10% and 22%, respectively. The structural elements present in the polysaccharide produced by GtfX-ΔNΔC were further identified by making use of COSY, TOCSY, ROESY and ^{13}C–^{1}H HSQC spectra (Fig. S8). Detailed interpretations of 2D NMR spectra are included in the Supplementary material and the chemical shifts of protons and carbons of the differently substituted Glc*p* residues are presented in Table S1. The results revealed the presence of 7 differently substituted Glc*p*

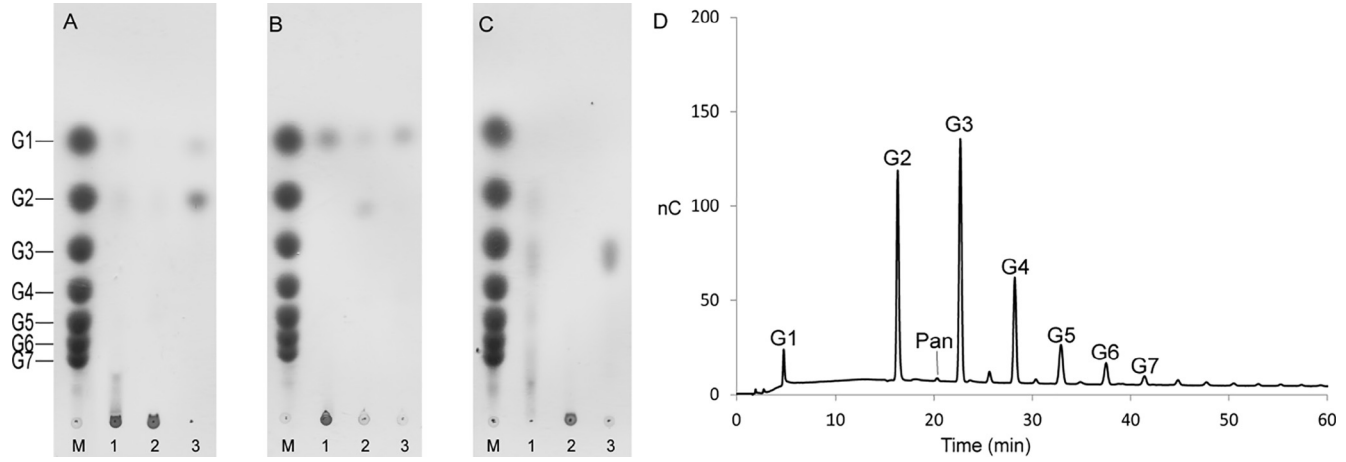

Fig. 5. TLC analysis of *Aspergillus oryzae* α-amylase (A), *Chaetomium erraticum* dextranase (B) and *Klebsiella planticola* pullulanase M1 (C) digestion of polysaccharides produced by incubation of GtfX-ΔNΔC and GtfY-ΔNΔC of *L. aviarius* subsp. *aviarius* DSM 20655 with amylose V. (D) HPAEC analysis of *Klebsiella planticola* pullulanase M1 digestion of polysaccharides produced by incubation of GtfX-ΔNΔC of *L. aviarius* subsp. *aviarius* DSM 20655 with amylose V. 1: GtfX-ΔNΔC polysaccharide; 2: GtfY-ΔNΔC polysaccharide; 3: positive control for α-amylase (amylose V), dextranase (dextran) and pullulanase M1 (pullulan) digestion, respectively; M: standards; G1: glucose; G2-G7: malto-oligosaccharides of DP2-7;Pan: panose.

residues [**A**: -(1 → 4)-α-D-Glc*p*-(1 → 4)-; **B**: α-D-Glc*p*-(1 → 4)-; **C**: -(1 → 6)-α-D-Glc*p*-(1 → 4)-; **D**: -(1 → 4,6)-α-D-Glc*p*-(1 → 4)-; **E**: -(1 → 4)-α-D-Glc*p*-(1 → 6)-**D**; **F**: -(1 → 4)-α-D-Glc*p*-(1 → 6)-**C**; **G**: α-D-Glc*p*(1 → 6)-]. The percentages of different structural elements in the polysaccharide produced by GtfX-ΔNΔC were deduced from the methylation analysis and the integration of (α1→4) and (α1→6) linkages in the ^{1}H NMR spectrum, allowing us to construct a composite polysaccharide model (Fig. S9).

The structures of the polysaccharides produced by GtfX-ΔNΔC and GtfY-ΔNΔC were further analyzed by enzymatic hydrolysis (Fig. 5). Firstly, α-amylase of *Aspergillus oryzae* was used to detect successive (α1→4) linkages, as it cleaves these in an endolytic mode. Under the conditions used, amylose V was completely hydrolyzed to glucose and maltose; in contrast, the polysaccharides produced by GtfX-ΔNΔC and GtfY-ΔNΔC were relatively resistant to α-amylase digestion (Fig. 5A). In the digested GtfX-ΔNΔC products, only small amounts of glucose, maltose and high molecular mass oligosaccharides were detected, while digested GtfY-ΔNΔC products contained very minor amounts of glucose and maltose. Secondly, dextranase of *Chaetomium erraticum* treatment of the GtfX-ΔNΔC and GtfY-ΔNΔC products was performed to confirm the presence of successive (α1→6) linkages (Fig. 5B). The polysaccharides produced by GtfX-ΔNΔC were also resistant to the digestion by dextranase of *C. erraticum* and only small amounts of glucose were detected in the digestion mixture, probably resulting from the terminal (α1→6) linkages in the polysaccharides. The polysaccharide produced by GtfY-ΔNΔC, and the dextran positive control, were hydrolyzed to glucose and isomaltose. Thirdly, pullulanase M1 of *Klebsiella planticola* was used since it specifically hydrolyzes the (α1→6) linkage in (-)α-D-Glc*p*-(1→4)-α-D-Glc*p*-(1→6)- units present in either linear sections or at branch points (van Leeuwen, Kralj et al., 2008). The polysaccharides produced by GtfX-ΔNΔC were completely hydrolyzed by pullulanase M1 (Fig. 5**C**). HPAEC analysis showed that these polysaccharides were hydrolyzed mainly to MOS of DP2-6 (Fig. 5D), while small amounts of higher DP MOS (> DP6) were also detected. In contrast, the polysaccharides produced by GtfY-ΔNΔC were resistant to the pullulanase M1 digestion.

Taken together, our structural analysis shows that the polysaccharides produced by GtfY-ΔNΔC are similar to the IMMP products synthesized by GtfB of *L. reuteri* 121, composed of consecutive (α1→6) linked glucosyl units attached to the non-reducing end of (α1→4) linked MOS segments (Dobruchowska et al., 2012; Leemhuis et al., 2014). The mode of action of GtfY-ΔNΔC thus resembles that of other characterized GtfB-type 4,6-α-GTs. In contrast, the products synthesized by GtfX-ΔNΔC contain MOS segments of varying lengths interconnected by single (α1→6) linked glucosyl units both in linear segments and branch points. These products are similar to the reuteran produced by GtfA of *L. reuteri* 121 from sucrose (van Leeuwen, Kralj et al., 2008) and the reuteran-like polymer produced by GtfD of *Azotobacter chroococcum* NCIMB 8003 (Gangoiti, van Leeuwen, Vafiadi, & Dijkhuizen, 2016), but contain much higher amounts of branching units (22%). The fact that the highly branched α-glucans synthesized by GtfX-ΔNΔC are resistant to α-amylase digestion, offers great potential for converting starch into slowly digestible or resistant starch, which can be used as dietary fiber in the food industry.

3.6. Reaction progress of GtfX-ΔNΔC and GtfY-ΔNΔC with maltoheptaose and amylose V as substrates

To further study the mode of action of GtfX and GtfY, the reactions of GtfX-ΔNΔC and GtfY-ΔNΔC with maltoheptaose (Fig. S10) and amylose V (Fig. S11) were followed in time and the oligosaccharides formed were analyzed by HPAEC. At the initial stage (t = 10 min) of the reaction with maltoheptaose (slightly contaminated with maltohexaose), GtfX-ΔNΔC produced G2, G3, G4 and G5 as hydrolysis products. At the same time, products with retention times longer than the donor substrate G7 and different from higher DP MOS were identified, suggesting that GtfX-ΔNΔC catalyzed the transfer of MOS units (G2-G5) to MOS acceptor substrates with the formation of (α1→6) linkages. After 8 h of incubation, G7 was virtually depleted and G2 had accumulated as the main hydrolysis product. Almost no glucose was detected throughout the incubation, indicating that GtfX-ΔNΔC virtually did not catalyze the transfer of single glucosyl units. When GtfY-ΔNΔC was incubated with the G7 substrate, G6 and G1 products were detected initially (t = 10 min). After 2 h of incubation, G6 and G1 were the main products; minor amounts of G2, G3, G4 and G5 were detected as well. In the meantime, oligosaccharides with retention times longer or shorter than the donor substrate (G7) and clearly different in mobility from MOS were detected; these likely correspond to oligosaccharide products containing (α1→6) linkages. After 8 h of incubation, G7 was almost depleted. Together, these results suggest that GtfX-ΔNΔC and GtfY-ΔNΔC interact differently with donor substrates, resulting in different modes of action on MOS. GtfX-ΔNΔC catalyzes the transfer of MOS (above DP2) with the formation of mainly branched (α1→6) linkage while GtfY-ΔNΔC catalyzes the transfer of single glucosyl unit with the synthesis of successive (α1→6) linkages. These differences must originate from differences in their active site, related to the amino acid differences between the enzymes.

In a second incubation setup, only amylose V was used as substrate.

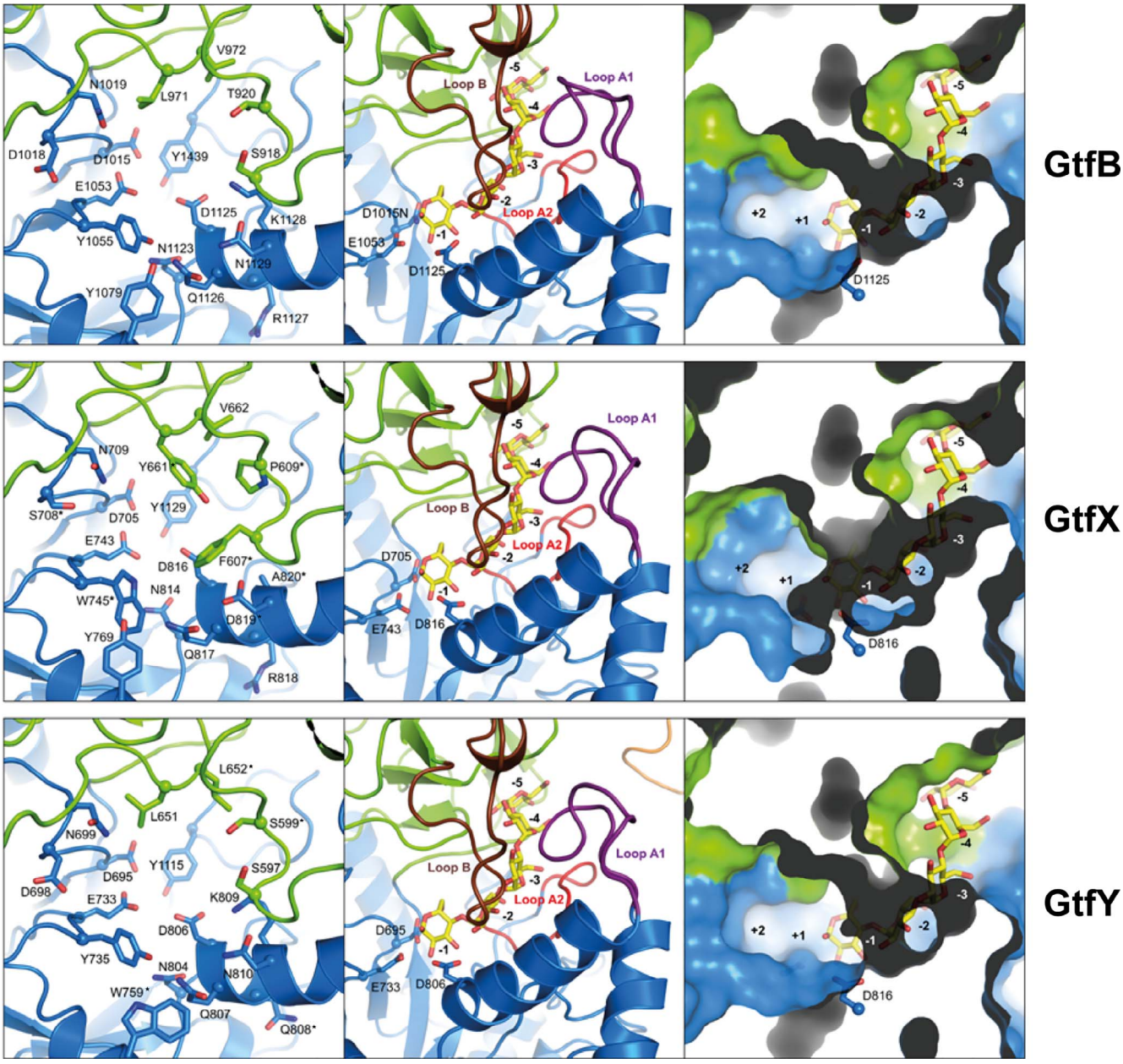

Fig. 6. Structural models of GtfX and GtfY, compared to the crystal structure of GtfB. The catalytic domain A is represented in blue, and domain B in green. Left panels show the active site region, with amino acid residues in GtfX and GtfY that are different from GtfB indicated with an asterisk. The middle panels show the three loops (loops A1 and A2 from domain A, loop B from domain B) that surround the maltopentaose bound in subsites −1 to −5 of GtfB; the architecture of the modeled loops of GtfX and GtfY is similar to that of the loops observed in GtfB. Nevertheless, adding the protein surfaces (right panels) shows that the shape of the active site of GtfX is different from that of GtfB and GtfY, including the acceptor substrate binding pocket (subsites +1, +2 etc.), due to the differences in amino acid residue side chains as depicted in the left panels. (For interpretation of the references to color in this figure legend, the reader is referred to the web version of this article.)

Here, GtfX-ΔNΔC released MOS with different DPs (predominantly maltose) in the initial stage (t = 5 min). Besides different DP MOS, products with clearly different retention times were detected after 8 h of incubation; likely these are oligosaccharide products with (α1→6) linkages resulting from the transglycosylase activity of GtfX-ΔNΔC. In addition, only very minor amounts of glucose were detected in the incubation mixture of GtfX-ΔNΔC with amylose V, as was seen with G7 as substrate. When GtfY-ΔNΔC was incubated with amylose V substrate, G1, G2 and G3 products were identified after 5 min. Small amounts of isomaltose and isomaltotriose were detected as transglycosylation products. After 8 h of incubation, large amounts of isomalto-oligosaccharides with different DP were detected, confirming the ability of GtfY-ΔNΔC to synthesize consecutive (α1→6) linkages.

3.7. Structural modeling of GtfX and GtfY

The Phyre server returned models of GtfX and GtfY comprising residues 447–1304 or 437–1290, respectively, corresponding to domains A, B, C and IV (Fig. 6). Of the 858 and 854 residues, 98% and 97% were modeled with a confidence > 90%, respectively. In both cases, the best scoring template was the crystal structure of the *L. reuteri* 121 GtfB-ΔNΔV mutant D1015N complexed with maltopentaose (PDB: 5JBF) (Bai et al., 2017); its sequence identity with GtfX and GtfY is 53% and 60% (for the modeled part), respectively.

Investigation of the overall architectures of the active site of GtfX and GtfY showed that they are very similar to that of GtfB of *L. reuteri* 121 (Bai et al., 2017). In GtfB, the loops A1, A2 and B surround the maltopentaose bound in subsites −1 to −5 and form a tunnel at

subsites −2 and −3. The predicted conformation of the corresponding loops in GtfX and GtfY is similar to that of the loops observed in GtfB and also form a tunnel that harbours donor subsites −2 and −3 (Fig. 6). At the cleavage site (subsites −1 and +1), GtfX and GtfY show high conservation with GtfB, in accordance with their common substrate specificity [cleavage of (α1→4) linkages in MOS type substrates]. Regarding the amino acids around acceptor substrate binding subsites (in motifs II-IV and in domain B), GtfY is more similar to GtfB; the only differences are S599 (corresponding to T920 in GtfB) in loop B, W759 (Y1079) in helix α4 and Q808 (R1127) in region IV, although the latter is far from the active site. In contrast, GtfX has more amino acid differences when compared to GtfB: S708 (D1018) in region II, W745 (Y1055) in region III, F607 (S918) and P609 (T920) in loop B, Y661 (L971) in domain B, and A820 (K1128) in region IV. Notably, three aromatic side chains (residues F607, Y661 and W745) are close to acceptor binding subsites, and likely cause the shape of the GtfX protein surface at acceptor subsites to be different from GtfB and GtfY. Thus, the differences and similarities at the amino acid level between GtfX and GtfY, compared to GtfB, reflect their different product specificities: GtfY and GtfB are similar, in accordance with their conserved 4,6-α-GT-type reaction specificity, while there are more pronounced differences between GtfX and GtfB, possibly contributing to the branching ability of GtfX. In this light, a notable feature of GtfX is the replacement of the conserved Tyr residue (Y1055) in motif III of all previously reported GtfB-like proteins by a Trp residue that is conserved in glucansucrase enzymes. This would suggest that the motif III Trp occurs in glucansucrases and 4,6-α-GT with branching activity, while the presence of a Tyr concurs only with those 4,6-α-GT that synthesize linear products. However, at the same time of the present study, we observed that another GtfB-like protein of *Lactobacillus reuteri* NCC 2613 from the Nestlé culture collection contains a motif III Tyr; yet it was also found to synthesize branched (α1→6) linkages similar to GtfX, albeit with a lower percentage of branch points (16%) (Gangoiti, van Leeuwen, Meng et al., 2017). GtfB of *L. reuteri* NCC 2613 shows some further sequence variations in regions II and IV, compared with other GtfB-like enzymes. Thus, the distinct product linkage specificity of GtfX cannot only be attributed to the aromatic residue in motif III, but likely results from the combined effects of amino acid residues around the acceptor binding subsites. This resembles the situation in glucansucrases, for which it was concluded that the linkage specificity is determined by the interplay of amino acid residues surrounding the acceptor substrate binding groove (Meng et al., 2016). The exact determinants and mechanism of GtfX in forming branched (α1→6) linkages remain to be studied.

It is also worth noting that the genes encoding GtfX and GtfY are adjacently located in the genome of *L. aviarius* subsp. *aviarius* DSM 20655. A similar situation has been reported in other *Lactobacillus* strains, e.g. the *gtfA* and *gtfB* gene pair in *L. reuteri* 121 encoding a GH70 glucansucrase and a 4,6-α-GT, respectively (Kralj et al., 2002; Kralj et al., 2011). It has been proposed that the evolution of GH70 glucansucrases and 4,6-α-GTs involves gene duplication events (Bai et al., 2017). The GtfX and GtfY gene pair may also have resulted from such an event, after which they evolved independently to acquire different activities by mutations. In our present study, we identified two GtfB-like proteins to be present in tandem. Interestingly, the conserved motif III of GtfX resembles that of GH70 glucansucrases with a tryptophan residue at position 1065 (GTF180 numbering) while the amino acid residues following the putative transition state stabilizer (region IV) are more similar to those of GH70 GtfB-like 4,6-α-GTs. In this light, GtfX may represent an intermediate between GtfB-like 4,6-α-GTs and GH70 glucansucrase enzymes, further completing the proposed evolutionary pathway starting from GH13 α-amylases, *via* GH70 glucanotransferases, to GH70 glucansucrases.

4. Conclusions

Glycoside hydrolase family 70 originally contained solely glucansucrase enzymes, catalyzing the synthesis of α-glucans from sucrose. Recently, GtfB-like 4,6-α-glucanotransferases were established as a new subfamily of GH70, predominantly forming consecutive (α1→6) linkages to yield linear isomalto/malto-oligosaccharide and polysaccharide products (IMMO and IMMP). Here, we report the identification and characterization of two GtfB-like 4,6-α-GTs (GtfX and GtfY) from *Lactobacillus aviarius* subsp. *aviarius* DSM 20655, which are present in tandem in the genome and show amino acid differences in conserved motifs I-IV compared to other GtfB-like proteins. Notably, GtfX contains a Trp residue in motif III, replacing the Tyr residue that is conserved in GtfB-like proteins and used as a fingerprint to identify putative GtfB-like proteins, discerning them from glucansucrases which possess a Trp at this position. Biochemical characterization revealed that GtfX has GtfB-like substrate specificity [active on (α1→4) glucans but not sucrose], but a product specificity that is clearly different from that of the *L. reuteri* 121 GtfB enzyme, resulting mainly in the formation of (α1→6) linked branches onto (α1→4) linked glucans. *In vitro* digestion analysis showed that the highly branched α-glucan produced by incubation of GtfX with amylose V is resistant to digestion by α-amylase. GtfY cleaves (α1→4) linkages in amylose and mainly forms consecutive (α1→6) linkages at the non-reducing end, similar to typical GtfB-like proteins (i.e. GtfB of *L. reuteri* 121). Structural modeling of GtfX and GtfY revealed that, with an overall conserved loop architecture, amino acid differences in motifs II-IV (including a non-canonical Trp in motif III) likely are responsible for the unique product specificity of GtfX. Our present study thus identified a GtfB-like enzyme in a *Lactobacillus* species able to synthesize highly branched isomalto-malto-oligosaccharide α-glucans, compared to the linear α-glucans synthesized by previously characterized GtfB-like 4,6-α-glucanotransferases. The structural determinants of GtfX's distinct product specificity remain to be investigated in detail. Nevertheless, the present study deepens our insights into the structure-function relationships of GtfB-like enzymes and offers great potential to synthesize α-amylase resistant α-glucans from starch as soluble dietary fibers.

Acknowledgements

This work was financially supported by China Postdoctoral Science Foundation-2017M622186 and the Fundamental Research Funds of Shandong University-2017TB0010 (to XM), and by the University of Groningen (to JG, SSvL, TP and LD).**Conflict of interest**

The authors declared no conflict of interest.

Appendix A. Supplementary data

Supplementary data associated with this article can be found, in the online version, at http://dx.doi.org/10.1016/j.foodchem.2018.01.154.

References

Badel, S., Bernardi, T., & Michaud, P. (2011). New perspectives for Lactobacilli exopolysaccharides. *Biotechnology Advances, 29*(1), 54–66.

Bai, Y., Gangoiti, J., Dijkstra, B. W., Dijkhuizen, L., & Pijning, T. (2017). Crystal structure of 4,6-α-glucanotransferase supports diet-driven evolution of GH70 enzymes from α-amylases in oral bacteria. *Structure, 25*(2), 231–242.

Bai, Y., van der Kaaij, R. M., Leemhuis, H., Pijning, T., van Leeuwen, S. S., Jin, Z., et al. (2015). Biochemical characterization of the *Lactobacillus reuteri* glycoside hydrolase family 70 GTFB type of 4,6-α-glucanotransferase enzymes that synthesize soluble dietary starch fibers. *Applied and Environment Microbiology, 81*(20), 7223–7232.

Brison, Y., Pijning, T., Malbert, Y., Fabre, E., Mourey, L., Morel, S., et al. (2012). Functional and structural characterization of α-(1→2) branching sucrase derived from DSR-E glucansucrase. *Journal of Biological Chemistry, 287*(11), 7915–7924.

Bultema, J. B., Kuipers, B. J., & Dijkhuizen, L. (2014). Biochemical characterization of mutants in the active site residues of the β-galactosidase enzyme of *Bacillus circulans* ATCC 31382. *FEBS Open Bio, 4*, 1015–1020.

Ciucanu, I., & Kerek, F. (1984). A simple and rapid method for the permethylation of carbohydrates. *Carbohydrate Research, 131*(2), 209–217.

Côté, G. L., & Skory, C. D. (2014). Effects of mutations at threonine-654 on the insoluble glucan synthesized by *Leuconostoc mesenteroides* NRRL B-1118 glucansucrase. *Applied Microbiology and Biotechnology, 98*(15), 6651–6658.

Dobruchowska, J. M., Gerwig, G. J., Kralj, S., Grijpstra, P., Leemhuis, H., Dijkhuizen, L., et al. (2012). Structural characterization of linear isomalto-/malto-oligomer products synthesized by the novel GTFB 4,6-α-glucanotransferase enzyme from *Lactobacillus reuteri* 121. *Glycobiology, 22*(4), 517–528.

Gangoiti, J., van Leeuwen, S. S., Gerwig, G. J., Duboux, S., Vafiadi, C., Pijning, T., et al. (2017). 4,3-α-Glucanotransferase, a novel reaction specificity in glycoside hydrolase family 70 and clan GH-H. *Scientific Reports, 7*, 39761.

Gangoiti, Joana, van Leeuwen, S. S., Meng, X., Duboux, S., Vafiadi, C., Pijning, T., Dijkhuizen, L. (2017). Mining novel starch-converting Glycoside Hydrolase 70 enzymes from the Nestlé Culture Collection genome database: The *Lactobacillus reuteri* NCC 2613 GtfB. Scientific Reports, 7, 9947.

Gangoiti, J., van Leeuwen, S. S., Vafiadi, C., & Dijkhuizen, L. (2016). The Gram-negative bacterium *Azotobacter chroococcum* NCIMB 8003 employs a new glycoside hydrolase family 70 4,6-α-glucanotransferase enzyme (GtfD) to synthesize a reuteran like polymer from maltodextrins and starch. *Biochimica et Biophysica Acta (BBA) – Bioenergetics, 1860*(6), 1224–1236.

Giffard, P. M., & Jacques, N. A. (1994). Definition of a fundamental repeating unit in *Streptococcal* glucosyltransferase glucan-binding regions and related sequences. *Journal of Dental Research, 73*(6), 1133–1141.

Hellmuth, H., Wittrock, S., Kralj, S., Dijkhuizen, L., Hofer, B., & Seibel, J. (2008). Engineering the glucansucrase GTFR enzyme reaction and glycosidic bond specificity: Toward tailor-made polymer and oligosaccharide products. *Biochemistry, 47*(25), 6678–6684.

Kelley, L. A., Mezulis, S., Yates, C. M., Wass, M. N., & Sternberg, M. J. (2015). The Phyre2 web portal for protein modeling, prediction and analysis. *Nature Protocol, 10*(6), 845–858.

Kralj, S., Grijpstra, P., van Leeuwen, S. S., Leemhuis, H., Dobruchowska, J. M., van der Kaaij, R. M., et al. (2011). 4,6-α-Glucanotransferase, a novel enzyme that structurally and functionally provides an evolutionary link between glycoside hydrolase enzyme families 13 and 70. *Applied and Environment Microbiology, 77*(22), 8154–8163.

Kralj, S., van Geel-Schutten, I. G. H., Dondorff, M. M. G., Kirsanovs, S., van der Maarel, M. J. E. C., & Dijkhuizen, L. (2004). Glucan synthesis in the genus *Lactobacillus*: Isolation and characterization of glucansucrase genes, enzymes and glucan products from six different strains. *Microbiology, 150*(11), 3681–3690.

Kralj, S., van Geel-Schutten, I. G. H., Rahaoui, H., Leer, R. J., Faber, E. J., van der Maarel, M. J. E. C., et al. (2002). Molecular characterization of a novel glucosyltransferase from *Lactobacillus reuteri* strain 121 synthesizing a unique, highly branched glucan with α-(1→4) and α-(1→6) glucosidic bonds. *Applied and Environment Microbiology, 68*(9), 4283–4291.

Kralj, S., van Geel-Schutten, I. G. H., van der Maarel, M. J. E. C., & Dijkhuizen, L. (2004). Biochemical and molecular characterization of *Lactobacillus reuteri* 121 reuteransucrase. *Microbiology, 150*(7), 2099–2112.

Kumar, S., Stecher, G., & Tamura, K. (2016). MEGA7: Molecular evolutionary genetics analysis version 7.0 for bigger datasets. *Molecular Biology and Evolution, 33*(7), 1870–1874.

Leemhuis, H., Dijkman, W. P., Dobruchowska, J. M., Pijning, T., Grijpstra, P., Kralj, S., et al. (2013). 4,6-α-Glucanotransferase activity occurs more widespread in *Lactobacillus* strains and constitutes a separate GH70 subfamily. *Applied Microbiology and Biotechnology, 97*(1), 181–193.

Leemhuis, H., Dobruchowska, J. M., Ebbelaar, M., Faber, F., Buwalda, P. L., van der Maarel, M. J., et al. (2014). Isomalto/malto-polysaccharide, a novel soluble dietary fiber made via enzymatic conversion of starch. *Journal of Agriculture and Food Chemistry, 62*(49), 12034–12044.

Leemhuis, H., Pijning, T., Dobruchowska, J. M., Dijkstra, B. W., & Dijkhuizen, L. (2012). Glycosidic bond specificity of glucansucrases: On the role of acceptor substrate binding residues. *Biocatalysis and Biotransformation, 30*(3), 366–376.

Leemhuis, H., Pijning, T., Dobruchowska, J. M., van Leeuwen, S. S., Kralj, S., Dijkstra, B. W., et al. (2013). Glucansucrases: Three-dimensional structures, reactions, mechanism, α-glucan analysis and their implications in biotechnology and food applications. *Journal of Biotechnology, 163*(2), 250–272.

MacGregor, E. A., Jespersen, H. M., & Svensson, B. (1996). A circularly permuted α-amylase-type α/β-barrel structure in glucan-synthesizing glucosyltransferases. *FEBS Letters, 378*(3), 263–266.

Meng, X., Gangoiti, J., Bai, Y., Pijning, T., Van Leeuwen, S. S., & Dijkhuizen, L. (2016). Structure-function relationships of family GH70 glucansucrase and 4,6-alpha-glucanotransferase enzymes, and their evolutionary relationships with family GH13 enzymes. *Cellular and Molecular Life Sciences, 73*(14), 2681–2706.

Meng, X., Pijning, T., Dobruchowska, J. M., Gerwig, G. J., & Dijkhuizen, L. (2015). Characterization of the functional roles of amino acid residues in acceptor binding subsite +1 in the active site of the glucansucrase GTF180 enzyme of *Lactobacillus reuteri* 180. *Journal of Biological Chemistry, 290*(50), 30131–30141.

Meng, X., Pijning, T., Tietema, M., Dobruchowska, J. M., Yin, H., Gerwig, G. J., et al. (2017). Characterization of the glucansucrase GTF180 W1065 mutant enzymes producing polysaccharides and oligosaccharides with altered linkage composition. *Food Chemistry, 217*, 81–90.

Monchois, V., Willemot, R.-M., & Monsan, P. (1999). Glucansucrases: Mechanism of action and structure-function relationships. *FEMS Microbiology Reviews, 23*(2), 131–151.

Monsan, P., Bozonnet, S., Albenne, C., Joucla, G., Willemot, R.-M., & Remaud-Siméon, M. (2001). Homopolysaccharides from lactic acid bacteria. *International Dairy Journal, 11*(9), 675–685.

Moulis, C., Joucla, G., Harrison, D., Fabre, E., Potocki-Vèronése, G., Monsan, P., et al. (2006). Understanding the polymerization mechanism of glycoside-hydrolase family 70 glucansucrases. *Journal of Biological Chemistry, 281*(42), 31254–31267.

Naessens, M., Cerdobbel, A., Soetaert, W., & Vandamme, E. J. (2005). *Leuconostoc* dextransucrase and dextran: Production, properties and applications. *Journal of Chemical Technology and Biotechnology, 80*(8), 845–860.

Ryan, P. M., Ross, R. P., Fitzgerald, G. F., Caplice, N. M., & Stanton, C. (2015). Sugar-coated: Exopolysaccharide producing lactic acid bacteria for food and human health applications. *Food Function, 6*(3), 679–693.

Studier, F. W. (2014). Stable expression clones and auto-induction for protein production in *E. coli*. *Methods in Molecular Biology, 1091*, 17–32.

van Leeuwen, S. S., Kralj, S., van Geel-Schutten, I. G. H., Gerwig, G. J., Dijkhuizen, L., & Kamerling, J. P. (2008a). Structural analysis of the α-D-glucan (EPS35-5) produced by the *Lactobacillus reuteri* strain 35-5 glucansucrase GTFA enzyme. *Carbohydrate research, 343*(7), 1251–1265.

van Leeuwen, S. S., Leeflang, B. R., Gerwig, G. J., & Kamerling, J. P. (2008b). Development of a ^{1}H NMR structural-reporter-group concept for the primary structural characterisation of α-D-glucans. *Carbohydrate Research, 343*(6), 1114–1119.

Vuillemin, M., Claverie, M., Brison, Y., Severac, E., Bondy, P., Morel, S., et al. (2016). Characterization of the first α-(1→3) branching sucrases of GH70 family. *Journal of Biological Chemistry, 291*(14), 7687–7702.

Vujičić-Žagar, A., Pijning, T., Kralj, S., López, C. A., Eeuwema, W., Dijkhuizen, L., et al. (2010). Crystal structure of a 117 kDa glucansucrase fragment provides insight into evolution and product specificity of GH70 enzymes. *Proceedings of National Academy Science of United states of America, 107*(50), 21406–21411.

Waterhouse, A. M., Procter, J. B., Martin, D. M., Clamp, M., & Barton, G. J. (2009). Jalview Version 2–a multiple sequence alignment editor and analysis workbench. *Bioinformatics, 25*(9), 1189–1191.

Zannini, E., Waters, D. M., Coffey, A., & Arendt, E. K. (2015). Production, properties, and industrial food application of lactic acid bacteria-derived exopolysaccharides. *Applied Microbiology and Biotechnology, 100*(3), 1121–1135.